Journal of Power Sources 187 (2009) 156–164

Contents lists available at ScienceDirect

Journal of Power Sources

journal homepage: www.elsevier.com/locate/jpowsour

Characterization of flooding and two-phase flow in polymer electrolyte membrane fuel cell stacks

G. Karimi[a,*], F. Jafarpour[a], X. Li[b]

[a] Department of Chemical and Petroleum Engineering, Shiraz University, Shiraz 7134851154, Iran
[b] Department of Mechanical and Mechatronics Engineering, University of Waterloo, Waterloo, Ontario, Canada N2L 3G1

ARTICLE INFO

Article history:
Received 23 May 2008
Received in revised form
14 September 2008
Accepted 19 October 2008
Available online 5 November 2008

Keywords:
PEM fuel cell
stack
Water management
Flooding;
Flow network analysis
Mathematical modeling

ABSTRACT

A partially flooded gas diffusion layer (GDL) model is proposed and solved simultaneously with a stack flow network model to estimate the operating conditions under which water flooding could be initiated in a polymer electrolyte membrane (PEM) fuel cell stack. The models were applied to the cathode side of a stack, which is more sensitive to the inception of GDL flooding and/or flow channel two-phase flow. The model can predict the stack performance in terms of pressure, species concentrations, GDL flooding and quality distributions in the flow fields as well as the geometrical specifications of the PEM fuel cell stack. The simulation results have revealed that under certain operating conditions, the GDL is fully flooded and the quality is lower than one for parts of the stack flow fields. Effects of current density, operating pressure, and level of inlet humidity on flooding are investigated.

1. Introduction

Polymer electrolyte membrane (PEM) fuel cells convert the chemical energy of hydrogen and oxygen directly and efficiently into electrical energy and are widely regarded as an alternative power source for stationary co-generation units, automotive and portable applications [1,2]. The main characteristics of PEM fuel cells are classified as (a) those that produce water as a byproduct; (b) those having higher efficiency when compared with heat engines; (c) those that operate at low temperatures (up to 90 °C) allowing a fast start-up; and (d) those using a solid polymer as the electrolyte, which reduces concerns related to construction, transportation, and safety.

In a PEM fuel cell, hydrogen and oxygen react electrochemically to water, producing electricity and heat. For the proper operation of a PEM fuel cell, both thermal and water management are critical to prevent the fuel cell system from overheating and performance deterioration [3]. If there is not enough water, the membrane becomes dehydrated and its resistance to proton conduction increases sharply [4]. On the other hand, if too much water is present, flooding may occur, and the pores of the gas diffusion layer, GDL, may be filled by liquid water, blocking the transport of reactants to the reaction sites, resulting in a serious performance drop, particularly at high current densities [5,6].

The problem of water management and transport in PEM fuel cells has been the subject of several theoretical and experimental studies. Bernardi [7] was the first to propose a one-dimensional model in order to study water management and to identify the humidification conditions which induce either the dehydration of the membrane or excessive flooding. Some other models were derived from the first principle, taking into account heat management [8], mass transport in the gas diffusion electrode [9], or to introduce a different treatment of the electrochemical reaction [10]. Bernardi et al. [11] and Springer et al. [12] also presented a one-dimensional model to investigate the factors that limit cell performance and to elucidate the mass transport mechanism within the complex network of gas, liquid and solid phases constituting the gas diffusion electrode. The molar changes along the gas flow channels are taken into consideration. Shimpalee et al. [13] investigated the performance of a 200-cm^2 PEM fuel cell with serpentine flow fields at various gas flow path lengths in terms of distributions in the local temperature, water content, and current density. They concluded that the shorter path length gives more uniform current density distribution and less condensed liquid water than the longer path. Liu et al. [14] studied membrane hydration and elec-

* Corresponding author. Tel.: +98 711 230 3071; fax: +98 711 647 4619.
E-mail addresses: ghkarimi@shirazu.ac.ir, gkarimi@engmail.uwaterloo.ca (G. Karimi).

0378-7753/$ – see front matter © 2008 Elsevier B.V. All rights reserved.
doi:10.1016/j.jpowsour.2008.10.108

Nomenclature

Nomenclature

A	cross-sectional area (m^2)
C	molar concentration ($mol\,m^{-3}$)
C_f	wall friction coefficient
d_h	flow channel hydraulic diameter (m)
D	diffusion coefficient ($m^2\,s^{-1}$)
D_h	manifold hydraulic diameter (m)
F	Faraday constant (96485 $C\,mole^{-1}$)
h	mass transfer coefficient ($m\,s^{-1}$)
H	bipolar plate effective height (m)
J	cell current density ($A\,m^{-2}$)
l	flow channel length (m)
L	gas diffusion layer thickness (m)
m	mass (kg)
N	number of cells/loops/inlets/outlets/flow channels/turns
$\dot{N}$	molar flow rate ($mol\,s^{-1}$)
$\dot{N}''$	molar flux ($mol\,m^{-2}\,s^{-1}$)
P	pressure (Pa)
Re	Reynolds number
RH	relative humidity (%)
Sh	Sherwood number
$\mathcal{S}$	stoichiometry
T	stack temperature (K)
V	average velocity ($m\,s^{-1}$)
W	bipolar plate effective width (m)
x	thermodynamic quality

Greek letters

δ	thickness (m)
Δ	difference
ϵ	fraction of flooded GDL
θ	flow direction convention
λ	electroosmotic drag coefficient
μ	viscosity ($N\,s\,m^{-2}$)
ρ	density ($kg\,m^{-3}$)
ϕ	porosity (%)

Subscripts/superscrpts

BD	back diffusion
c	cathode/flow channel
cell	fuel cell
CV	control volume
eff	effective
f	flooded
EO	electroosmotic drag
G	gas
GDL	gas diffusion layer
Gen	generation
i	loop number
in	inlet
inlets	inlet number(s)
j	segment number
loop	loop
L	liquid
min	minimum
Max	maximum
outlet	outlet number
Out	outlet
stack	stack
total	total
TP	two-phase
w	water
b	bulk
w-g	water–gas

trode flooding by developing a 2D partial flooding model in which size distributions are assigned for the hydrophobic and hydrophilic pores of the GDL. The liquid water produced is considered to condense in hydrophilic and hydrophobic pores in sequence if the water vapor pressure is higher than the condensation pressure for the pores. The model results, under a wide range of operating conditions, have shown reasonable agreement with the experimental data. Experimentally, two-phase flow and transport of reactants and products in the cathode of a transparent PEM fuel cell were studied by Tuber et al. [15]. Images of water formed inside the cathode gas channels are presented to explain the phenomenon of water flooding. Effects of air stoichiometry, temperature, air humidity and different characteristics of diffusion layers are discussed. Liu et al. [16] and Weng et al. [17] studied water flooding and two-phase flow in cathode flow channels with different flow paths using transparent PEM fuel cells. Their experimental results indicated the significant effects of flow channel patterns and cathode gas stoichiometry on water removal efficiency and cell performance.

Almost all of the research conducted to study flooding in PEM fuel cells experimentally or theoretically, are limited to a single cell. The goal of this research is to add to the knowledge base to produce generic design guidelines for operating conditions and flow fields that can be applied to PEM fuel cell stacks, consisting of a more practical number of cells. It is assumed that the development of these design techniques could be a useful tool for the improvement of water management, and shed further light on its effect on fuel cell stack performance. To this end, a partially flooded GDL model is proposed and solved simultaneously with a stack flow network model to estimate the design and operating conditions under which water flooding could be initiated in a PEM fuel cell stack. The model was applied to the cathode side of a stack, which is more sensitive to the inception of GDL flooding and/or flow channel two-phase flow. The model presented here is an extended version of a recent model [18,19] which can predict the stack performance in terms of pressure, species concentrations, GDL flooding, and quality distributions in the flow fields as well as the geometrical specifications of the PEM fuel cell stack.

2. Model formulation

A schematic diagram of a typical PEM fuel cell stack is shown in Fig. 1. The individual cells, referred to as membrane electrode assemblies (MEAs), are composed of a membrane electrolyte sandwiched in the middle of the cell, and typically contains catalyst and microporous gas diffusion layers along with gaskets as a single integrated unit. One of the gas diffusion layers is referred to as the anode, the other as the cathode. The catalyst layer at the anode separates hydrogen molecules into protons and electrons. The membrane permits ion transfer (protons), requiring the electrons to flow through an external circuit before recombining with protons and oxygen at the cathode to form water. This migration of electrons produces useful work.

In practice, oxygen, pure or in air, enters the cathode side of the stack through the main inlet(s), travels along the inlet manifold and is distributed into the flow channels or fields. From the flow fields, O_2 diffuses through the GDL towards the cathode–membrane interface where it is reduced to form water and heat which are

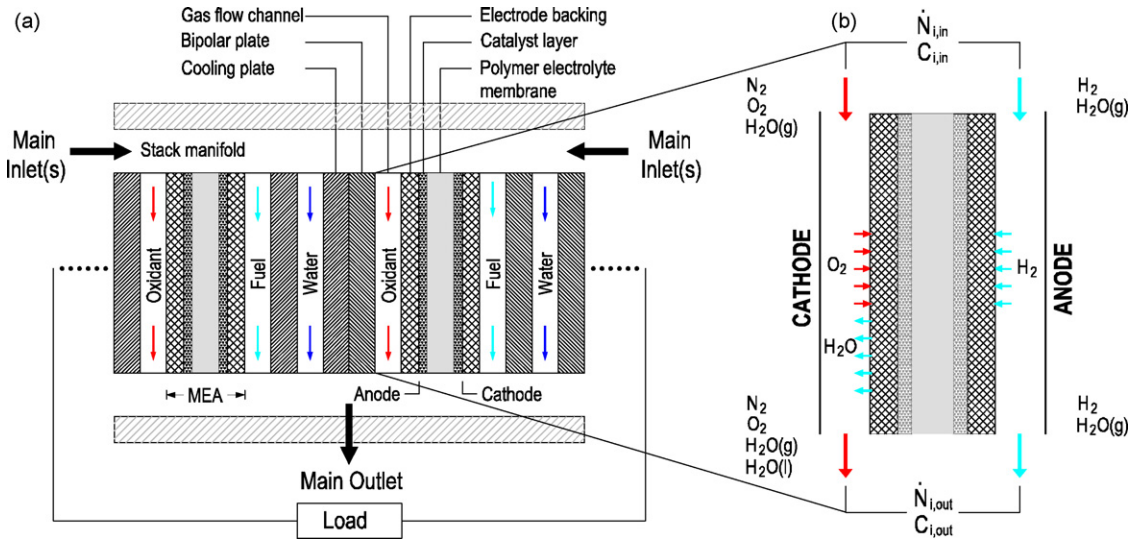

Fig. 1. Schematic of a PEM fuel cell stack.

then removed from the system. Water can also be added to the cathode side due to the electroosmotic drag and be transferred from the cathode to the anode due to back diffusion. The simultaneous water and oxygen transfer, in conjunction with significant pressure variations in the cathode bipolar plate flow channels can lead to situations where liquid water flood the GDL, partially or completely, and even deposit on the flow fields. This phenomenon hinders the O_2 transport to the reaction sites, and could stop fuel cell operation if the extent of flooding is significant. The focus of the present work is to develop a thermo-hydraulic model based on conservation laws to predict the state of flooding in the stack. The mathematical model consists of two parts; a stack flow model and a partially flooded GDL model, which are explained as follows.

2.1. Stack flow model

The cross-section of a PEM fuel cell stack was shown in Fig. 1. Fig. 2 illustrates, in greater detail, the structure of a typical cathode bipolar plate with inlet and outlet manifolds and three flow channels arranged in a serpentine configuration. To model the extent of GDL flooding and the possibility of two-phase flow distribution in the stack, the complex oxidant flow paths consisting of the main inlet(s), inlet and outlet manifolds and the gas flow channels can be reduced into a graphical flow network as depicted in Fig. 3, where each MEA is surrounded by the manifolds and the flow channels. The top manifold supplies the oxidant stream to the flow channels and the unreacted oxygen, accompanied by water and nitrogen, exit into the bottom manifold, collect and leave the stack.

The oxygen reduction starts at the beginning of the flow channels right after the oxygen, protons and electrons are brought into contact in the catalytic layer. The reaction rates vary along the flow channels as the species composition and pressure change. In a recent study, Karimi et al. [18] employed a simplified control volume approach (six control volumes per cell in total) to predict the average species concentrations throughout the fuel cell stack for a wide variety of inlet-outlet topologies. In the present work, the flow paths are divided into a larger number of control volumes in the flow channels to capture, in greater detail, the variations in the species concentrations, local pressures, and the possibility of GDL flooding and/or two-phase flow inception in the flow fields. The new network model consists of an arbitrary number of loops (associated with each cell), with each loop comprised of M segments: two in the inlet and outlet manifolds, and $(M-2/2)$ in each flow channel. The interfaces at which any two segments meet are represented by nodes (•) as illustrated in Fig. 3. Within each control volume it is assumed that the pressure and compositions are uniform. Mass transfers due to electrochemical reactions are considered to take place uniformly along the flow channels, resulting in uniform current distribution.

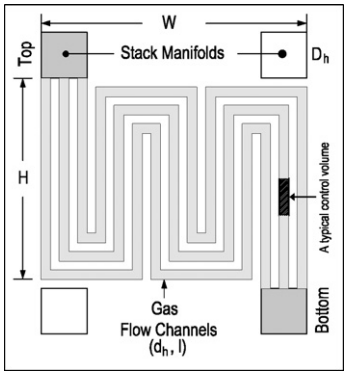

Fig. 2. Illustration of a bipolar plate with serpentine flow field and three channels per plate.

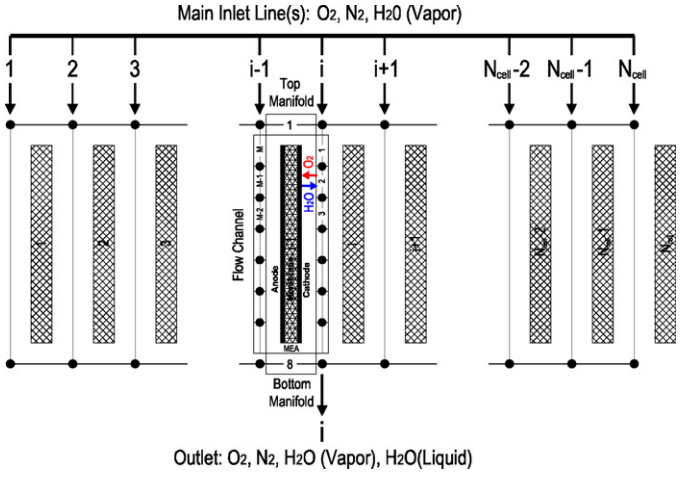

Fig. 3. Graphical representation of the stack flow network model.

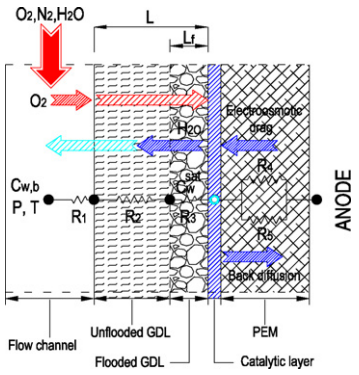

Fig. 4. Graphical representation of the partially flooded GDL model.

The total molar flow rate of O_2 entering the cathode side of the stack can be determined by

$$\dot{N}_{O_2}^{stack} = \frac{\mathcal{S}_c N_{cell} J A_{cell}}{4F} \quad (1)$$

where $\mathcal{S}_c$ is the cathode stoichiometry, N_{cell} is the total number of fuel cells in the stack, J is the current density and A_{cell} is the active area of a unit cell, respectively. Total inlet molar flow rate can be calculated by adding nitrogen and water vapor to the oxygen molar flow rate. The maximum amount of water vapor coming into the cathode corresponds to 100% relative humidity.

The distribution of incoming components in the stack is governed by the conservation laws. The local species concentrations are calculated based on the amount of water produced electrochemically, and the amount that is transferred by diffusion and electroosmotic drag in the catalytic layer. This will be discussed in the next section. In order to satisfy the conservation of energy, the sum of pressure changes around each of the loops, *i*, should be

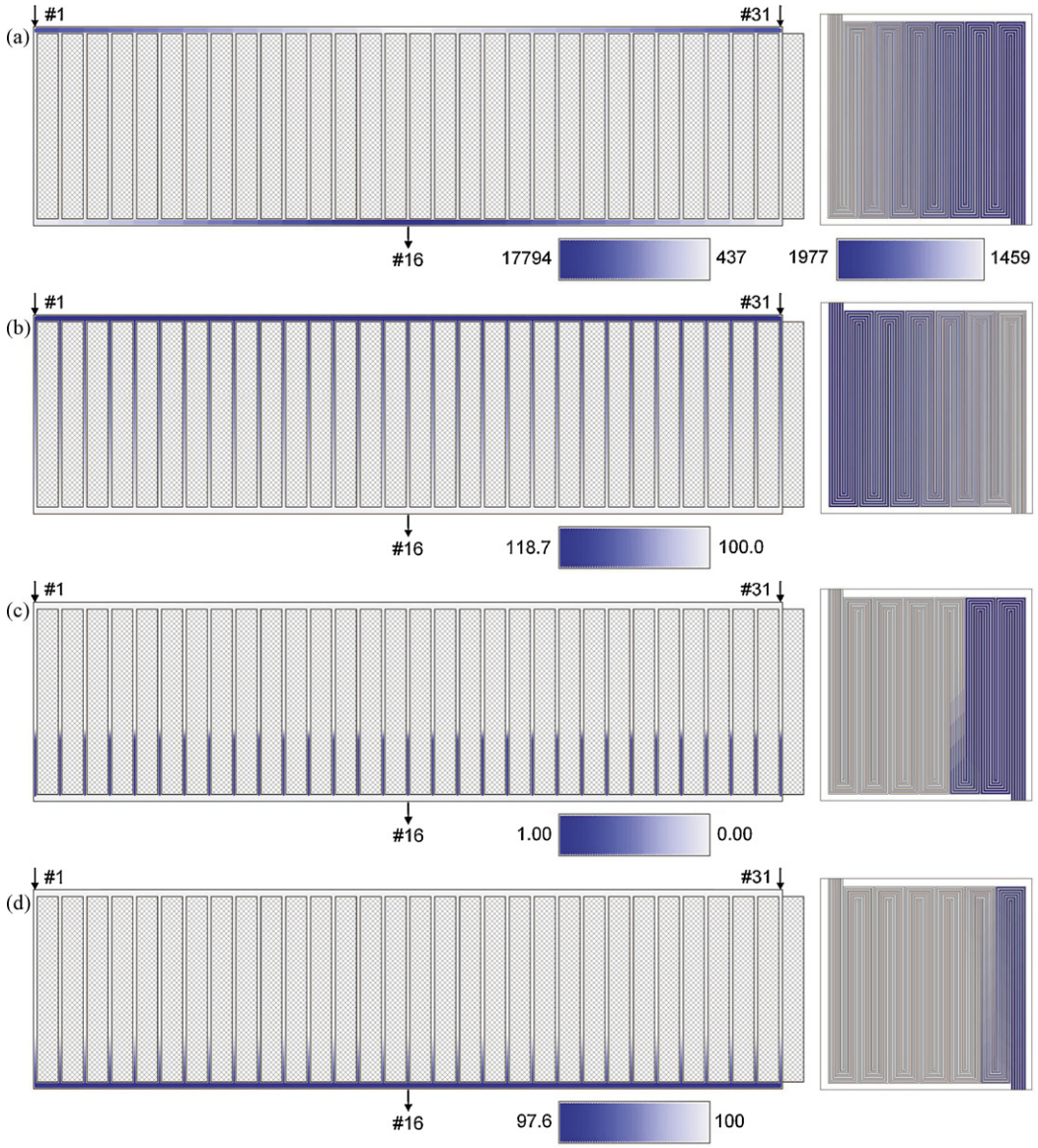

Fig. 5. Spatial variations of operating parameters in the cathode side of a PEM fuel cell stack (a) Reynolds number, (b) Pressure, (c) GDL flooding ϵ, and (d) mixture quality x. The flow channels shown on the right represent the distribution of parameters in the central bipolar plate (#16) in the stack shown on the left. ($J = 5000\,A\,m^{-2}$, $T = 353\,K$, $P_{out} = 1$ atm, RH_{in}=80%).

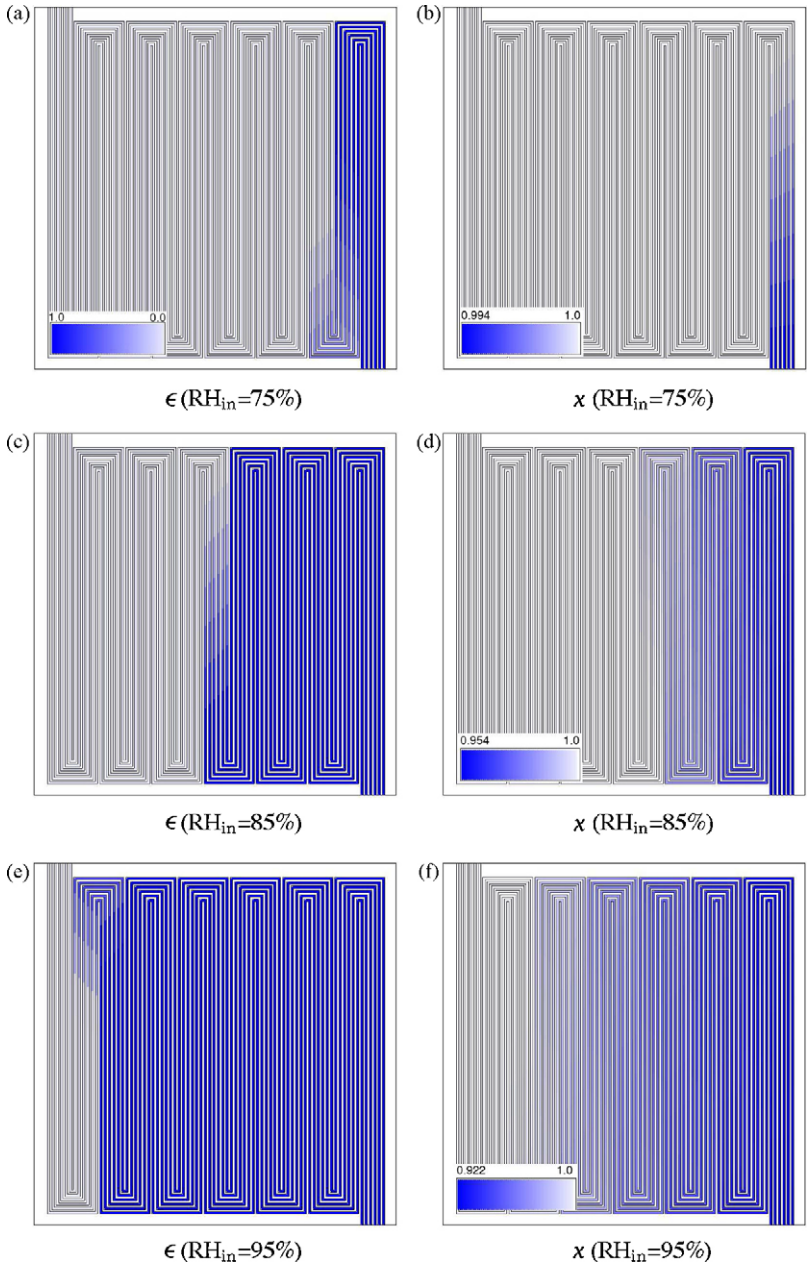

Fig. 6. Effect of level of air humidification on the GDL flooding ϵ and the resulting mixture quality x in the bipolar flow channels ($J = 5000\,\mathrm{A\,m^{-2}}$, $T = 353\,\mathrm{K}$, $P_{\mathrm{out}} = 1$ atm).

zero,

$$\sum_{j=1}^{M} \theta_{i,j} \Delta P_{i,j} = 0 \qquad (i = 1, 2, 3, s, N_{\mathrm{loop}}) \tag{2}$$

where $\theta_{i,j}$ is a sign convention representing the direction of flow in the segment j of loop i. $\theta_{i,j}$ is considered to be +1 when fluid flows in a clockwise direction and −1 if the direction is reversed. The frictional pressure drop in a segment j of the loop i can be calculated from

$$\Delta P_{\mathrm{f},i,j} = C_{\mathrm{f},i,j} \frac{l_{i,j}}{D_{\mathrm{h},i,j}} \frac{\rho_{i,j} V_{i,j}^2}{2} \tag{3}$$

where $l_{i,j}$ and $D_{\mathrm{h},i,j}$ are the segment (or control volume) length and hydraulic diameter, $\rho_{i,j}$ is the fluid average density, and $V_{i,j}$ is the average velocity in the segment j of the loop i. The friction coefficient, $C_{\mathrm{f},i,j}$, is a function of the Reynolds number defined based on the hydraulic diameter

$$\mathrm{Re}_{i,j} = \frac{\rho_{i,j} V_{i,j} D_{\mathrm{h},i,j}}{\mu_{i,j}} \tag{4}$$

The physical properties ρ and μ are calculated depending on whether single- or two-phase flow prevails in the flow channels. For two-phase flow in mm-sized flow channels, Pehlivan et al. [20] showed experimentally that the conventional homogeneous model can be used to predict two-phase pressure drops reasonably well. It is also to be noted that at high mixture qualities, the liquid volume fractions in the flow fields are extremely small, so the error associated with the homogeneous model should be minimal. The

Table 1
Parameters and properties used in the present PEM fuel cell stack model.

Component	Parameter	Value
Bipolar plate	W	0.15 m
	H	0.15 m
	l	1.8 m
	d_h	1 mm
	D_h	10 mm
	N_c	6
Stack	N_{cells}	31
	N_{inlets}	2 (#1, #31)
	N_{outlet}	1 (#16)
	T	353 K
	P_{out}	1–2 atm
	RH_{in}	50–100%
	J	1000–10000 A m^{-2}
	S_c	2.0
	λ	0.4
GDL	δ_{GDL}	250 μm
	ϕ_{GDL}	40%

two-phase physical properties are calculated from:

$$\rho_{TP} = \left(\frac{x}{\rho_G} + \left(\frac{1-x}{\rho_L}\right)\right)^{-1}, \qquad \mu_{TP} = \left(\frac{x}{\mu_G} + \left(\frac{1-x}{\mu_L}\right)\right)^{-1} \tag{5}$$

where x is the mixture quality defined as the mass fraction of gas in the flow fields:

$$x = \frac{m_G}{m_{total}} \tag{6}$$

Subscripts TP, G, and L denote "two-phase", "gas" and "liquid", respectively.

2.2. Partially flooded GDL model

Fig. 4 illustrates different mechanisms for water transport through a segment of the cathode side in a PEM fuel cell stack. The network of mass transfer resistances and potentials are also included in this figure. The partially flooded GDL model presented here is based on the following assumptions: (1) Oxygen reduction occurs in the catalytic layer with negligible thickness, hence, the cathode flooding, if any, starts at the interface of the catalytic layer and grows inside the GDL towards the flow fields. (2) The hampering of O_2 diffusion through the cell results in increased overpotentials. (3) The combined electroosmotic drag and back diffusion effects are considered to be uniform along the catalytic layer. The net effect is determined by considering that the gas stream leaving the anode outlet is fully humidified. (4) The GDL pore structure is considered to be uniform throughout the cell. If GDL is fully flooded, the extra water enters the flow channels. The liquid water moves along with the gas stream uniformly and its volume is negligible. (5) The stack operates at constant temperature. With these assumptions in place, the extent of GDL flooding is governed by the balance of water generation, the net water transport due to the electroosmotic drag and back diffusion, and the rate at which water is removed by the cathode gas. The maximum possible water transfer through the GDL can be represented by

$$\dot{N}''_{Max} = \frac{C_w^{sat} - C_{w,b}}{\frac{L}{D_{w-g}^{eff}} + \frac{1}{h_{w,b}}} \tag{7}$$

where C_w^{sat} is the water saturation concentration at the cell operating temperature, $C_{w,b}$ is the local bulk concentration in the flow channel, L is the GDL thickness, D_{w-g}^{eff} is the effective diffusivity for water vapor transfer through the GDL, and $h_{w,b}$ is the local mass transfer coefficient. $h_{w,b}$ can be estimated by considering mass transfer in a fully developed laminar flow through a three-sided adiabatic square duct with constant mass flux applied at one surface and no-flux applied at the others [21]:

$$Sh = \frac{h_{w,b} D_h}{D_{w-g}} = 2.7 \tag{8}$$

Now, if the rate of water production at the catalytic layer–GDL interface is less than or equal to $\dot{N}''_{Max}$, water can be easily removed from the system, otherwise the GDL will be flooded with extra water in liquid form. Under steady-state conditions the local fraction of the flooded GDL, ϵ, can be estimated as

$$\epsilon = \frac{L_f}{L} \quad \text{where} \quad L_f = L - \left(\frac{C_w^{sat} - C_{w,b}}{\dot{N}''_{H_2O}} - \frac{1}{h_{w,b}}\right) D_{w-g}^{eff} \tag{9}$$

where L_f is the thickness of the flooded GDL. $\dot{N}''_{H_2O}$ can be calculated from:

$$\dot{N}''_{H_2O} = \frac{\dot{N}_{H_2O}}{A_{CV}} \quad \text{and} \quad \dot{N}_{H_2O} = \dot{N}_{Gen} + \underbrace{\dot{N}_{EO} - \dot{N}_{BD}}_{\text{Net interaction with anode}} \tag{10}$$

where

$$\dot{N}_{Gen} = \frac{JA_{CV}}{2F} \tag{11}$$

where A_{CV} is the control volume surface area available for mass transfer.

Eq. (9) can be solved in conjunction with the recently developed flow network solution algorithm [18,19] to obtain the distribution in the extent of water flooding in the GDL under a variety of geometrical and operating conditions.

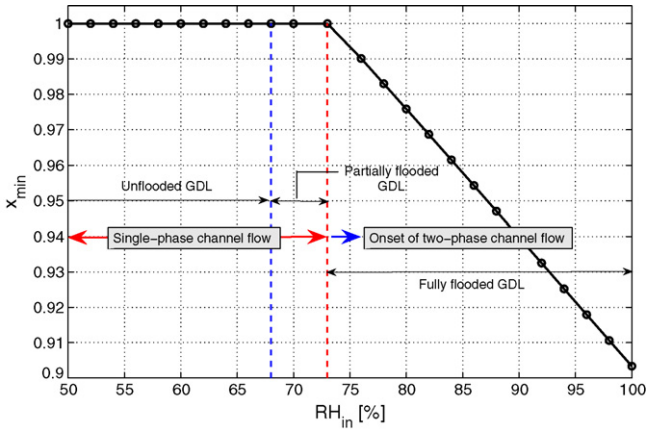

Fig. 7. Effect of inlet air humidification on the minimum x in bipolar flow channels ($J = 5000$ A m^{-2}, $T = 353$ K, $P_{out} = 1$ atm).

3. Numerical procedure

The flow network solution algorithm adopted in this work is based on the modified Hardy Cross method that has recently been reported [18]. Numerical solution begins with assigning a temporary flow direction to the flow network. The sum of the molar flow rates from all the inlets (with known compositions) is then divided uniformly among the gas flow channels. The molar flow rates and compositions in the downstream sections of the flow channels are calculated by subtracting the consumed reactants and adding the produced or transported components. Water transport through the membrane due to the combined effects of electroosmotic drag and back diffusion is also considered. The conservation of mole equation is used to calculate the molar flow rates in the inlet and outlet manifolds based on the predefined directions and the assumed molar

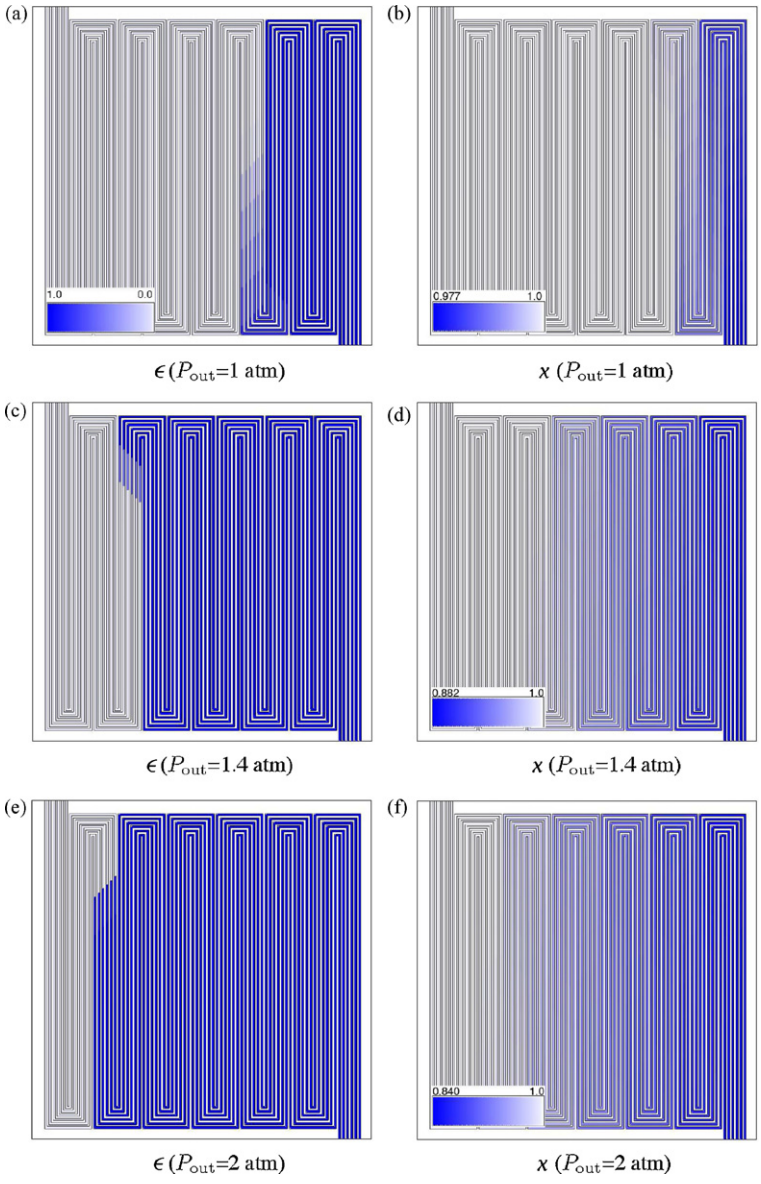

Fig. 8. Effect of the stack pressure on the GDL flooding and the resulting mixture quality in the bipolar flow channels ($J = 5000\,A\,m^{-2}$, $T = 353\,K$, RH_{in}=80%).

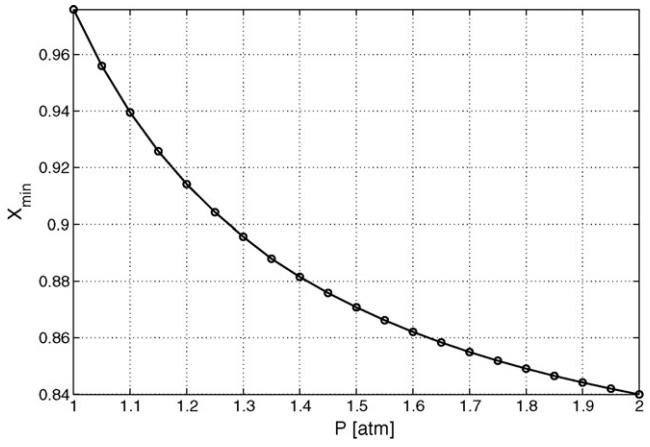

Fig. 9. Effect of stack pressure on the minimum x in bipolar flow channel ($J = 5000\,A\,m^{-2}$, $T = 353\,K$, RH_{in}=80%).

flow rates in the flow channels. To satisfy the conservation of energy equation, the pressure drop is calculated for each segment based on the local mixture quality and appropriate pressure drop equations. The procedure is repeated until correct flow directions and molar flow rates are obtained for the whole flow network. The local species concentrations are used in Eq. (9) to calculate the fraction of GDL that is flooded with liquid water, ϵ. If GDL is fully flooded at some point along the flow fields, the extra water is added into the cathode stream, changing the local quality, x, and hence the resulting pressure drop is calculated based on two-phase flow properties defined in Eq. (5).

4. Results and discussion

The input parameters for the fuel cell and stack flow model are classified as operating and design parameters. The design parameters are the fuel cell size, stack manifold and flow channel dimensions and configuration. Operating parameters include the stack current density, temperature, pressure, stoichiometry and the

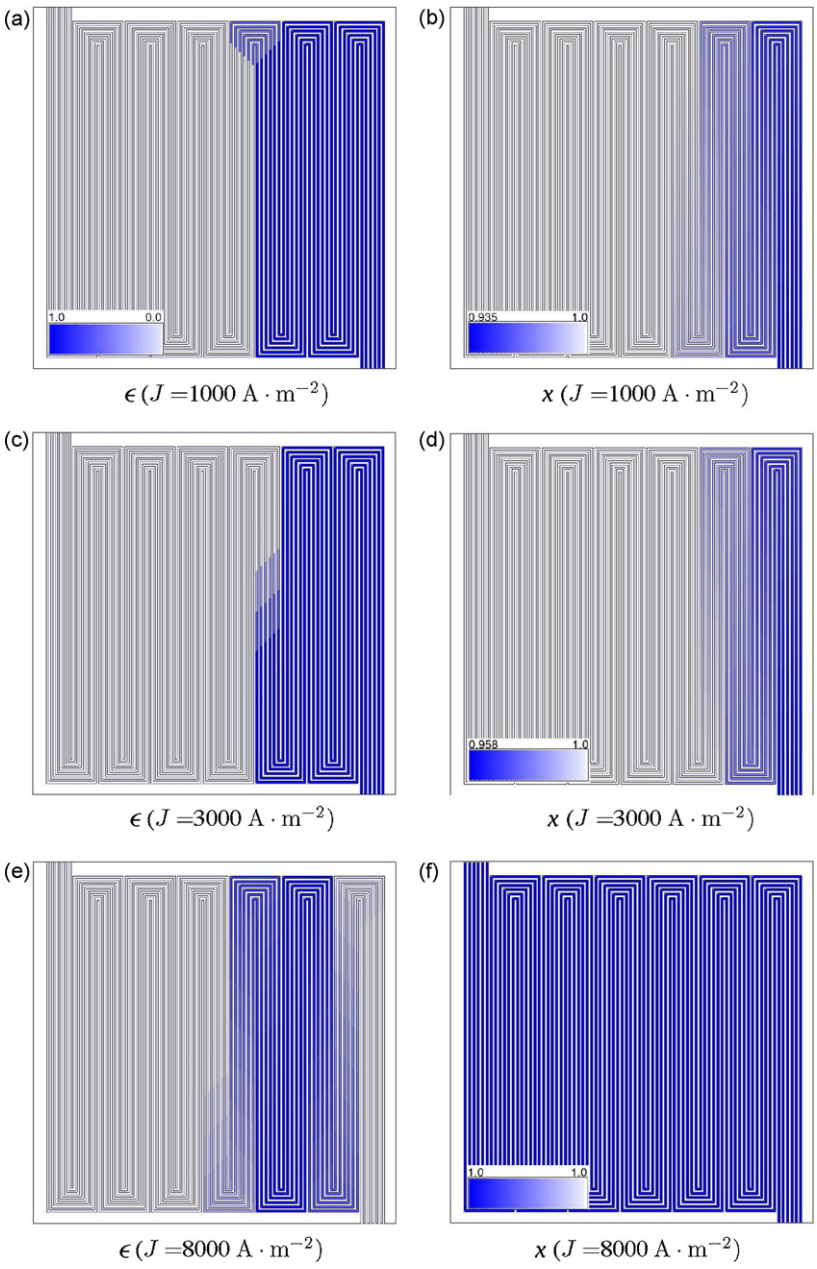

Fig. 10. Effect of the current density on the GDL flooding and the resulting mixture quality in the bipolar flow channels (T = 353 K, P_{out} = 1 atm, RH_{in}=80%).

reactant composition at the stack inlet. Table 1 lists a summary of the operating and relevant design parameters used in the present study for the cathode side of the PEM fuel cell stack.

The stack is considered to be composed of 31 cells, with two oxidant inlets at the endpoints of the inlet manifold (#1 and #31) and one outlet at the middle of the exit manifold (#16). This symmetric double-inlet-single-outlet configuration was shown to be the most effective scheme with minimal cell-to-cell voltage variations and parasitic losses [18]. Humidified air at different pressures and water contents was injected into the stack.

Fig. 5a–d shows variations in different operating parameters in the cathode side of a fuel cell stack at a current density of 5000 A m^{-2}. The figures on the left side display an overall view of the stack consisting of the inlet and outlet manifolds and the flow channels. The figures on the right side show details of the operating parameters inside the central bipolar plate (#16) with three serpentine flow channels. Fig. 5a shows the variation of Re number in the manifolds and across the flow channels. The Reynolds number decreases along the inlet manifold from the endpoints towards the middle channels as the reactants are delivered to the flow channels. The flow division is almost uniform due to the large pressure drop in the flow channels compared with that of the inlet manifold, resulting in a linear reduction in the Reynolds number. This phenomenon is repeated for the outlet manifold as the unreacted O_2, N_2 and H_2O are collected and leave the stack. Inside the flow channels, Re number varies as the local velocity, density and viscosity change. However, the flow remains in the laminar region.

Pressure distribution in the stack is illustrated in Fig. 5b. There are two factors contributing to the pressure variation along the flow path in the stack. First, the total molar flow rate is increased along the flow channels because two moles of H_2O are produced for every mole of O_2 consumed in the catalytic layer; this will increase

the local pressure. Second, pressure along the channels is reduced due to friction. At constant current density, water concentration is increased along the flow channels. This increases the possibility of water flooding in the GDL and even condensation of water vapor inside the flow channels. The latter could initiate two-phase flow in the lower parts of the stack. This is evident from Fig. 5c and d where the percentage of flooded GDL, ϵ, and mixture quality, x, along the flow channels are depicted. As expected, the GDL must be completely flooded before the mixture qualities start to decrease from 1 (single-phase) to lower values (e.g. 0.97), for which the onset of two-phase flow in lower parts of the stack could be initiated. However, the resulting quality distributions in Fig. 5d are insufficient to incept a major two-phase flow in the stack. This is due to very large liquid-to-gas density ratio, which leads to gas fractions of greater than 99% in the flow channels.

Fig. 6a–f illustrates the effect of the level of air humidification on the GDL flooding and the resulting mixture quality in the bipolar flow channels. As seen from these figures, as the inlet air relative humidity, RH_{in}, is increased, a larger portion of the GDL will be flooded and lower qualities are observed in the flow channels. Although the extent of GDL flooding does have a significant effect on the mass transfer overpotential, the lower x values may not be important as pointed out earlier.

It is quite useful to estimate the minimum quality, x_{min}, which prevails in the bipolar flow channels and how the inlet air humidity, stack pressure and current density affect this value. In fact, x_{min} is a direct indication of the extent of GDL flooding because the GDL must be completely flooded before the x values drop below one. Fig. 7 indicates the effect of RH_{in} on the x_{min} in the flow channels. As seen from this figure, portions of GDL start to flood if the RH_{in} exceeds 68%. The flooded regions grow as RH_{in} increases and GDL is fully flooded when $RH_{in} = 73\%$. Numerical results showed that at inlet relative humidities of 70% and 72%, GDL was flooded by 5% and 92%, respectively. At larger RH_{in} values, the extra water permeates through the flow channels and results in lower x values. The minimum x observed for this case was about 90% when a fully humidified air enters the stack.

The effect of the stack pressure on the GDL flooding and the resulting quality in the bipolar flow channels are shown in Fig. 8a–f. As indicated, by increasing the stack pressure, the partial pressure of the produced water is augmented and water tends to condensate in the GDL pores. As a result, the quality of the gas flow is also decreased. Fig. 9 indicates that the stack operating pressure has a more noticeable effect on GDL flooding than the inlet air humidity. As shown in this figure, increasing the stack outlet pressure from 1 atm to 2 atm will result in a minimum x value of about 84%.

Fig. 10 a–f illustrates the effect of the stack current density on the GDL flooding and the resulting quality in the bipolar flow channels. By increasing the stack operating current density, a larger amount of oxidant stream needs to flow in the bipolar flow fields, resulting in significantly low pressures, particularly in the vicinity of the flow channel exits. The lower pressures there enhance water transport through the GDL, reducing the extent of flooding. The quality in the flow channels are also affected. Figs. 10 and 11 indicate that the possibility of GDL flooding and the inception of two-phase flow in the flow fields is reduced at high stack current densities.

The numerical results shown in Figs. 5–11 indicate the GDL in the cathode side of the PEM fuel cell stack can easily be flooded and the quality of gas flow in the flow fields could decrease from one. Although GDL flooding and the inception of two phase flow are among the common issues in PEM fuel cells and have been reported in numerous papers, the extent of these issues are alleviated by the heat of the reaction which is released during the oxygen reduction at the catalyst layer, and by significant reduction in the O_2 diffusion through the GDL. Also, as pointed out earlier, a minimum x value of about 84%, can not be responsible for the inception of two-phase flow in the system. Because the corresponding void fraction is estimated to be very close to 1 (e.g. 99.9%) for the worst case scenario reported here.

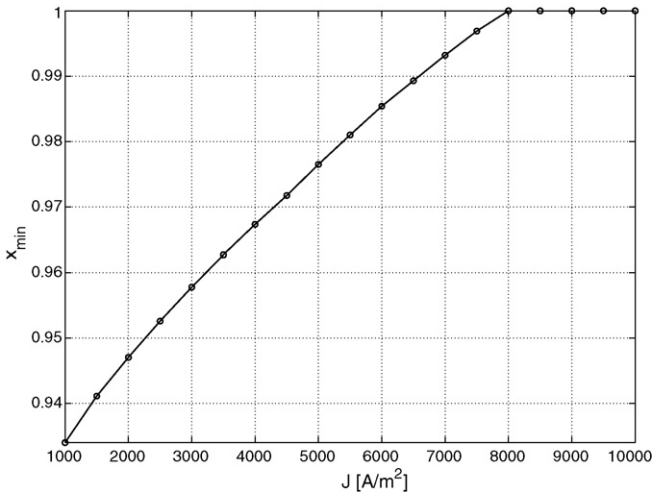

Fig. 11. Effect of operating current density on the minimum x in bipolar flow channels ($T = 353$ K, $P_{out} = 1$ atm, RH_{in}=80%).

5. Conclusions

Water management is one of the most critical issues for high-performance polymer electrolyte membrane (PEM) fuel cells. A partially flooded GDL model is proposed and used in conjunction with a cathode flow network model to predict the conditions under which the GDL could be flooded in a PEM fuel cell stack. Effects of current density, operating pressure, and level of inlet humidity on GDL flooding are studied. The simulation results have revealed that although under certain operating conditions the GDL is fully flooded, and water can be liquified in parts of the stack flow fields, the amount of the liquified water in the stack is not significant enough to cause a major pressure drop or an appreciable change in the species concentrations.

References

[1] C.K. Dyer, J. Power Sources 106 (2002) 31–34.
[2] C. Hebling, A. Heinzel, D. Golombowski, T. Meyer, M. Muller, M. Zedda, Proceedings of HYFORUM 2000, vol. II, München, Germany, 2000, pp. 383–393.
[3] L. You, H. Liu, Int. J. Heat Mass Transfer 45 (2002) 2277–2287.
[4] T.A. Zawodzinski, C. Derouin, S. Radzinski, R.J. Sherman, V.T. Smith, T.E. Springer, S. Gottesfeldet Jr., J. Electrochem. Soc. 140 (4) (1993) 1041–1047.
[5] J. Larminie, A. Dicks, Fuel Cell Systems Explained, 2nd ed., John Wiley and Sons, 2003.
[6] J.J. Baschuk, X. Li, J. Power Sources 86 (2000) 181–196.
[7] D.M. Bernardi, J. Electrochem. Soc. 137 (11) (1990) 3344–3350.
[8] T.V. Nguyen, R.E. White, J. Electrochem. Soc. 140 (8) (1993) 2178–2186.
[9] T.E. Springer, T.A. Zawodzinski, S. Gottesfeld, J. Electrochem. Soc. 138 (8) (1991) 2334–2342.
[10] G. Murgia, L. Pisani, M. Valentini, B.D. Aguanno, J. Electrochem. Soc. 149 (1) (2002) 31–38.
[11] D.M. Bernardi, M.K. Verbrugge, J. Electrochem. Soc. 139 (9) (1992) 2477–2491.
[12] T.E. Springer, M.S. Wilson, S. Gottesfeld, J. Electrochem. Soc. 140 (12) (1993) 3513–3526.
[13] S. Shimpalee, S. Greenway, J.W. Van Zee, J. Power Sources 160 (2006) 398–406.
[14] Z. Liu, Z. Mao, C. Wang, J. Power Sources 158 (2006) 1229–1239.
[15] K. Tuber, D. Pocza, C. Hebling, J. Power Sources 124 (2003) 403–414.
[16] X. Liu, H. Guoa, C. Maa, J. Power Sources 156 (2006) 267–280.
[17] F.B. Weng, A. Su, C.Y. Hsu, C.Y. Lee, J. Power Sources 157 (2006) 674–680.
[18] G. Karimi, J.J. Baschuk, X. Li, J. Power Sources 147 (2005) 162–177.
[19] G. Karimi, F. Jafarpour, X. Li, Cairo 10th International Conference on Energy and Environment, March 11–15, Luxor, Egypt, 2007.
[20] K. Pehlivan, I. Hassan, M. Vaillancourt, Appl. Thermal Eng. 26 (2006) 1506–1514.
[21] S. Kakac, R.S. Shah, W. Aung, Handbook of Single-phase Convective Heat Transfer, John Wiley and Sons, New York, 1987, pp. 3.45–349.